Al-Azhar University Civil Engineering Research Magazine (CERM)
Vol. (41) No. (2) April, 2019

Experimental And Analytical Study Of Reinforced Concrete Columns Confined By Smart Material Active And Passive External Stirrups

E. M. Atia 1, M. A. Alkersh 2, A. M. Hilal 3, M. Abdelrazik. 4
1 Lecturer Assistant, Department of Structural Engineering, Al Azhar University, Cairo, Egypt
2 Lecturer, Department of Structural Engineering, Al Azhar University, Cairo, Egypt
3 Associate Professor, Department of Structural Engineering, Al Azhar University, Cairo, Egypt
4 Professor, Department of Structural Engineering, Al Azhar University, Cairo, Egypt

الملخص:
يهدف هذا البحث الي دراسة سلوك الاعمدة الخرسانيه المسلحه المدعمه بكانات خارجية (سابقة الاجهاد وغير سابقة الاجهاد) من المواد الذكيه من خلال عدد من التجارب العمليه مع التركيز علي دراسة تاثير المسافة بين الكانات الخارجيه (سابقة الاجهاد وغير سابقة الاجهاد) وكذلك قوه داخليه متغيره علي حمل الكسر في العمود والانفعال في المواد الذكيه عند الكسر وكذلك عمل مقارنه بين النتائج العمليه والنتائج المحسوبه من الاكواد المختلفه وفي نهاية البحث تم عرض اهم النتائج والتوصيات .

1- Abstract

Shape Memory Alloys (SMA) ware used as external stirrups to confine Reinforced Concrete columns. The effect of spacing between external stirrups, tension force in the external stirrups and type of confinement (active or passive) on the behavior of strengthened reinforced concrete columns was studied. An experimental program consisting of three groups and a reference group was performed. A wide range parametric study was made. Strains were measured at different stages of loading. The load strain curves were plotted. The relation between each variable and the capacity of the column was plotted. The final results showed that the increase in the external stirrups spacing in case of both passive and active confinement caused the decrease of the capacity of columns strengthened with SMA, increase tension force in the external stirrups caused increase capacity of columns strengthened .

Keywords: SMA, Active or Passive Confinement, External Stirrups, Reinforced Concrete, Columns Strengthened.

2. Introduction

Recovering the original shape of the SMA after being deformed beyond its elastic limits through unloading is referred to as super-elasticity, and through heating is characterized as the Shape Memory Effect (SME). Under a stress-free state, loading the material in its martensitic form results in a linear elastic stress-strain response until the minimum de twinning stress (σ_s) is reached in Figure 1. After this point, the SMA experiences a yielding plateau due to a de twinning process characterized by a zone of large strains and low stiffness. The de twinning finish stress (σ_f) marks the completion of the de twinning process and is usually followed by an increase in the stiffness depending on the type of the SMA. At this stage, unloading the SMA would approach a state of zero stress with retained deformation in the material. Recovering the original un deformed state of the material occurs by heating the SMA above the austenite finish temperature (A_f). Subsequent cooling of the SMA would transform the material back to its martensitic state, and the entire cycle can be repeated Figure (1).

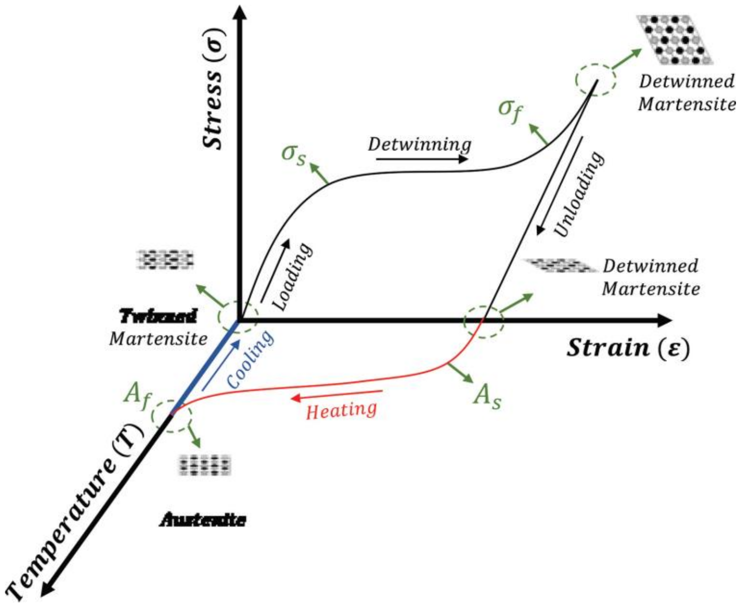

Figure 1 smart material effect

3. Experimental program

Sixteen RC columns with overall dimensions of 100 mm diameter, 700mm height were tested. The vertical longitudinal reinforcement of all specimen was 4 bars with diameter 10mm. The internal stirrups were 4mm diameter bars at 220mm spacing, additional three stirrups and one layer CFRP at 100mm beginning and end of column to avoid local failure. The external stirrups were (SMA plate U-shape) 2mm thickness, 20mm wide,380 mm length, 30mm beginning and end on the form of 90 degree angle and hole diameter 8mm in center of the angle. The specific parameter of each specimen was described in Table (1).

The test specimens were divided into three groups and a column reference depending on the spacing of transverse external stirrups as shown in Figure (2).

Column (reference) CR control column passive confined.

Group (1) consisted of five columns, spacing between external stirrups @ 60mm. Column (C11) was passively confined and temperature external stirrups smaller than 15 degree Celsius. Column (C12) was passively confined and temperature external stirrups bigger than 23 degree Celsius. Column (C13) was actively confined, temperature external stirrups bigger than 23 degree Celsius and tension of external stirrups by 2000 N. Column (C14) was actively confined, temperature external stirrups bigger than 23 degree Celsius and tension of external stirrups by 4000 N. Column (C15) was actively confined, temperature external stirrups bigger than 23 degree Celsius and tension of external stirrups by 6000 N.

Group (2) consisted of five columns, spacing between external stirrups @ 90mm. Column (C21) was passively confined and temperature external stirrups smaller than 15 degree Celsius. Column (C22) was passively confined and temperature external stirrups bigger than 23 degree Celsius. Column (C23) was actively confined, temperature external stirrups bigger than 23 degree Celsius and tension of external stirrups by 2000 N. Column (C24) was actively confined, temperature external stirrups bigger than 23 degree Celsius and tension of external stirrups by 4000 N. Column (C25) was actively confined, temperature external stirrups bigger than 23 degree Celsius and tension of external stirrups by 6000 N.

Group (3) consisted of five columns, spacing between external stirrups @ 120mm. Column (C31) was passively confined and temperature external stirrups smaller than 15 degree Celsius. Column (C32) was passively confined and temperature external stirrups bigger than 23 degree Celsius. Column (C33) was actively confined, temperature external stirrups bigger than 23 degree Celsius and tension of external stirrups by 2000 N. Column (C34) was actively confined, temperature external stirrups bigger than 23 degree Celsius and tension of external stirrups by 4000 N. Column (C35) was actively confined, temperature external stirrups bigger than 23 degree Celsius and tension of external stirrups by 6000 N.

A constant concrete mix was used in this research. The aimed concrete characteristic strength was 22.5 MPa.

One hydraulic jack was used with capacity 100 Ton. Figure (3) shows the general setup and the test frame.

Table 1 Specific parameter of each columns

Group	Column	Spacing external stirrups (mm)	Type of confinement	Temperature (°C)	Applied torque (N.mm)	Bolt pretension force(N)
reference	CR	0	--------	--------	--------	--------
1	C11	60	Passive	≤15	0	0
	C12	60	Passive	≥23	0	0
	C13	60	Active	≥23	$3.2x10^6$	2000
	C14	60	Active	≥23	$6.4\ x10^6$	4000
	C15	60	Active	≥23	$9.6\ x10^6$	6000
2	C21	90	Passive	≤15	0	0
	C22	90	Passive	≥23	0	0
	C23	90	Active	≥23	$3.2x10^6$	2000
	C24	90	Active	≥23	$6.4\ x10^6$	4000
	C25	90	Active	≥23	$9.6\ x10^6$	6000
3	C31	120	Passive	≤15	0	0
	C32	120	Passive	≥23	0	0
	C33	120	Active	≥23	$3.2x10^6$	2000
	C34	120	Active	≥23	$6.4\ x10^6$	4000
	C35	120	Active	≥23	$9.6\ x10^6$	6000

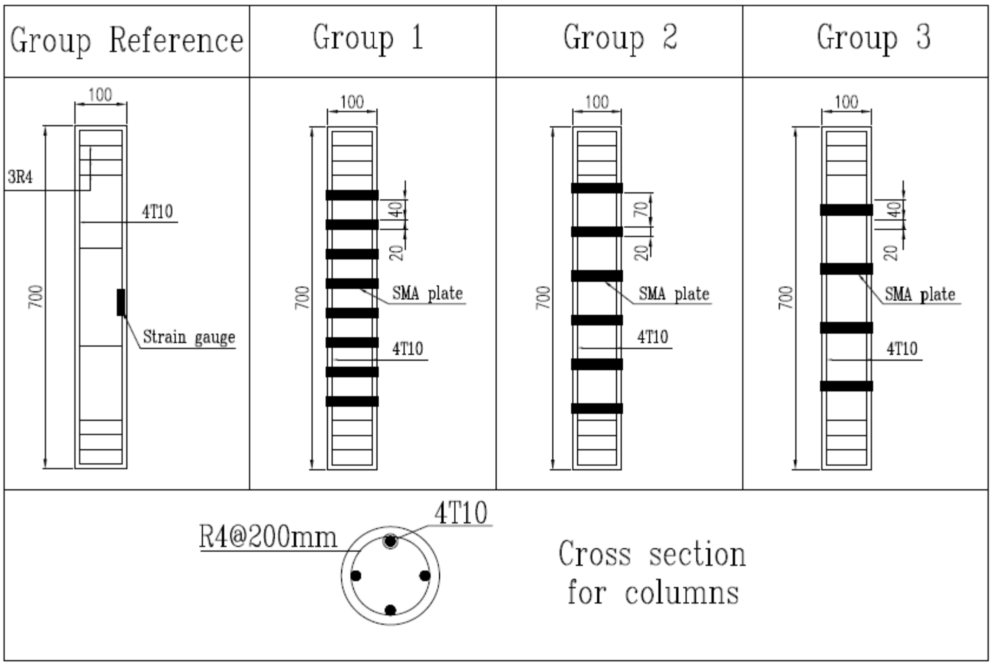

Figure 2 Details of reinforcement for all Groups

Figure 3 Testing Frame

4. Discussion of The Experimental Results

Form the observed behavior of the tested columns the following remarks were concluded:

4.1 Failure Load

The failure loads of the tested columns were compared with estimated failure loads due to failure according to (ACI -440-2R-08) and Egyptian Code of FRP (ECP-208) and compared active with passive external stirrups.

- ACI -440-2R-08

$$f'_{cc} = f'_{co}\left(-1.254 + 2.254\sqrt{\mathbf{1} + \frac{7.94 f'_l}{f'_{co}}} - 2\frac{f'_l}{f'_{co}}\right) \quad 1$$

$$f'_l = 1/2\ k_e\, \rho_s\, f_{yh} \quad 2$$

$$k_e = \frac{1-\left(\frac{s''}{2d_s}\right)^2}{1-\rho cc} \quad 3$$

$$\rho_s = \frac{A_{sp}*\pi*d_s}{\frac{\pi}{4}{d_s}^2*s} \quad 4$$

- ECP-208

$$f'_{cc} = f_{co}\left(2.25\sqrt{\mathbf{1} + \frac{9.875 f'_l}{f'_{co}}} - 2.5\frac{f'_l}{f'_{co}} - 1.25\right) \quad 5$$

$$\boldsymbol{f_1} = \frac{1}{2}\,\frac{1}{\gamma_f}\,\boldsymbol{k_e}\ \rho_s\ f_{yh} \quad 6$$

$$\boldsymbol{k_e} = \left(\mathbf{1} - \frac{(S-b_f)}{2D}\right)^2 < \mathbf{1} \quad 7$$

$$\rho_s = \frac{4*b_f*n*t_f}{S*D} \quad 8$$

Where: f'cc = the strength of confined concrete at failure, f'co = unconfined concrete compressive strength, f'l= effective lateral confining pressure, fyh= the yield strength of transverse reinforcement, ke = the confinement effective coefficient, ρcc = the ratio of the area of the axial steel to the area of the core of the section, s'' = the clear spacing between the spiral, ρs = the transverse reinforcement ratio, Asp = area of transverse reinforcement bar, ds = the diameter of the spiral between bar centers, s = the spacing between the spiral, γ_f= 1.3 (material strength reduction factor of the SMA), D = diameter of column, n = number of plies of SMA reinforcement, t_f = nominal thickness of one ply of SMA, b_f = width of the SMA.

Group 1 :

For C11 and C12 the analytical failure loads were smaller than the experimental failure loads by 2% and 5% in (ECP) and C11 equal (ACI) and C12 smaller by 1% in (ACI) respectively. Figures (4,5) show the comparison between experimental and analytical failure loads of C11 and C12.

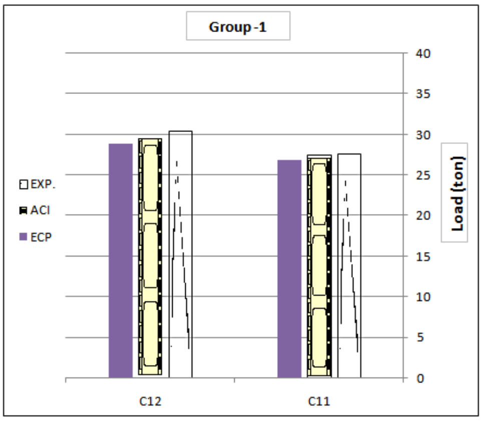

Figure 4 Cracks Pattern of C11,C12 **Figure 5 Failure Load of C11,C12**

For C13, C14 and C15 the experimental failure loads were bigger than C12 by 5%, 7% and 11% respectively. Figures (6,7) show the comparison between experimental failure loads of (C13,C14,C15 and C12).

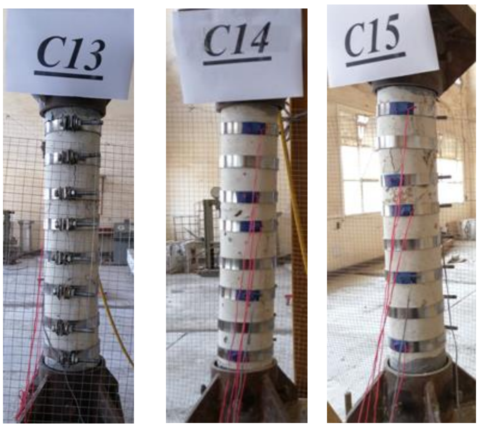

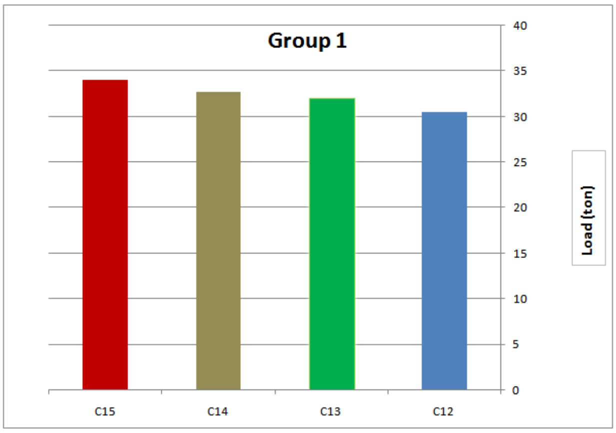

Figure 6 Cracks Pattern of C13,C14,C15 **Figure 7 Failure Load of C13,C14,C15 Comparison between active & passive**

Group 2 :

For C21 and C22 the analytical failure loads were smaller than the experimental failure loads by 2% and 7% in (ECP) and C21, C22 smaller by 3% and 6% in (ACI) respectively. Figures (8,9) show the comparison between experimental and analytical failure loads of C21 and C22.

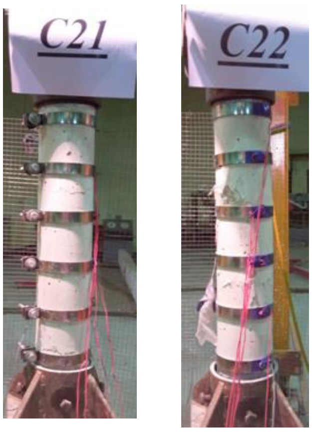

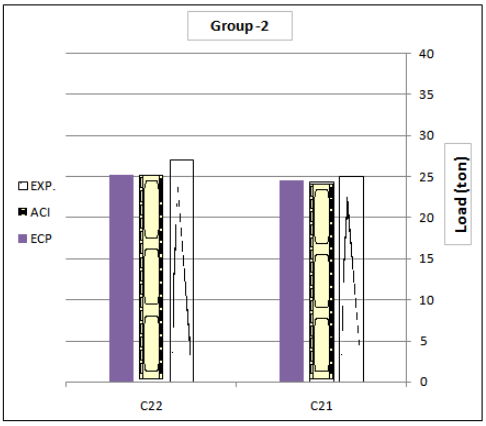

Figure 8 Cracks Pattern of C21,C22 **Figure 9 Failure Load of C21,C22**

For C23, C24 and C25 the experimental failure loads were bigger than C22 by 2%, 4% and 7% respectively. Figures (10,11) show the comparison between experimental failure loads of (C23,C24,C25 and C22).

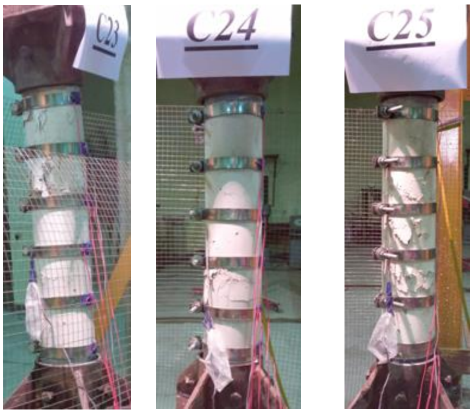

Figure 10 Cracks Pattern of C23, C24,C25

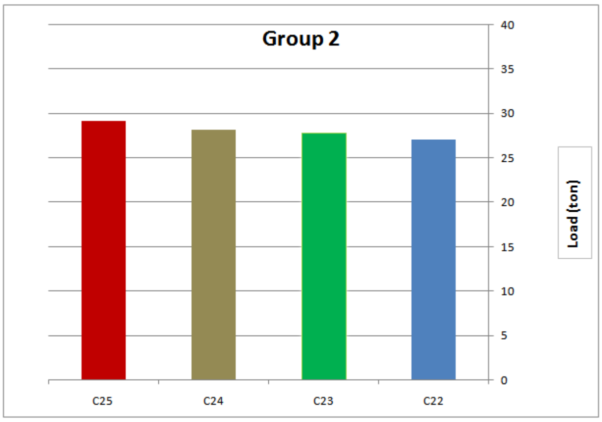

Figure 11 Failure Load of C23,C24,C25 Comparison between active & passive

Group 3 :

For C31 and C32 the analytical failure loads were smaller than the experimental failure loads by 2% and 3% in (ECP) and C31, C32 smaller by 3% and 2% in (ACI) respectively. Figures (12,13) show the comparison between experimental and analytical failure loads of C31 and C32.

Figure 12 Cracks Pattern of C31,C32

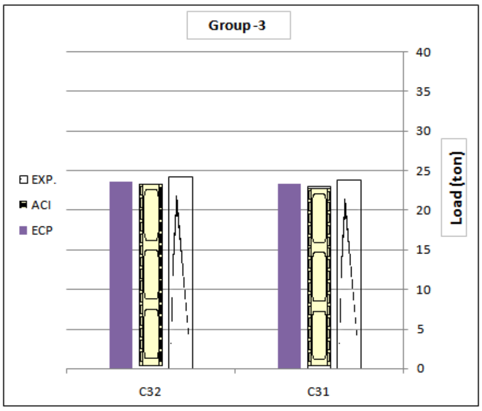

Figure 13 Failure Load of C31,C32

For C33, C34 and C35 the experimental failure loads were bigger than C32 by 3%, 5% and 7% respectively. Figures (14,15) show the comparison between experimental failure loads of (C33,C34,C35 and C32).

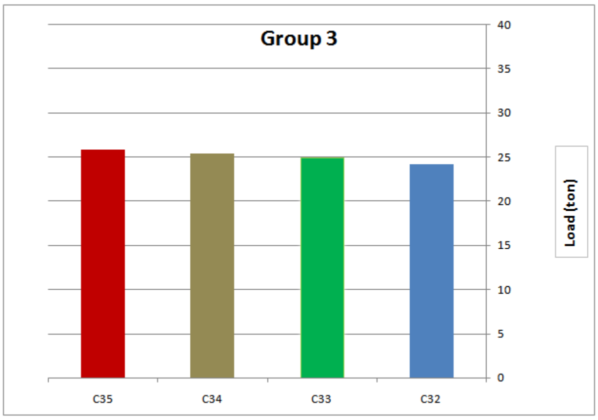

Figure 14 Cracks Pattern of C33, C34,C35

Figure 15 Failure Load of C33,C34,C35 Comparison between active & passive

Reference Group

For CR the analytical failure loads was bigger than the experimental failure load by 8% in (ECP) respectively and smaller by 8% in (ACI) respectively. Figures (16,17) show the comparison between experimental and analytical failure loads of CR.

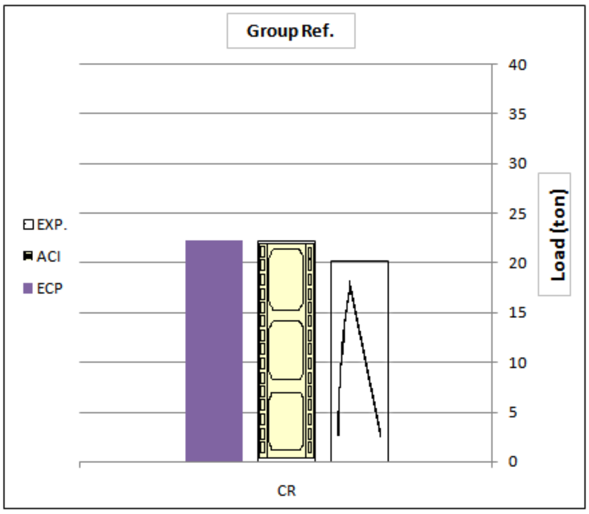

Figure 16 Cracks Pattern of Group Ref.

Figure 17 Failure Load of Group Ref.

The failure load for experimental, ACI and ECP for all columns are shown in Table(2).

Table (2) failure load for experimental, ACI and ECP results

Group	1					2					3					Ref.
Column	C11	C12	C13	C14	C15	C21	C22	C23	C24	C25	C31	C32	C33	C34	C35	CR
EXP. failure load	27.6	30.4	32.0	32.6	34.0	25.1	27.1	27.8	28.2	29.1	23.8	24.2	24.9	25.3	25.8	20.3
ACI. failure load	27.5	29.9	----	----	----	24.4	25.4	----	----	----	23.1	23.6	----	----	----	22.1
ECP. failure load	26.9	28.9	----	----	----	24.5	25.2	----	----	----	23.3	23.5	----	----	----	22.1

4.2 Steel Strains

The longitudinal steel strains were obtained from the electrical strain gauges. Figures (18) to (21) show the load steel strain curves, through the load history, for the all groups at the first third span section.

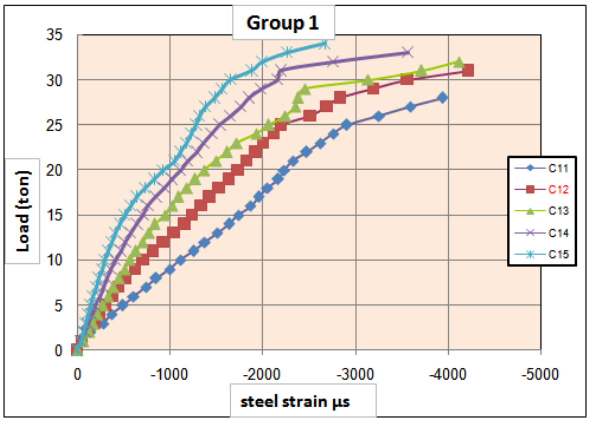

Figure 18 Comparison between longitudinal Steel strain at midpoint for group 1

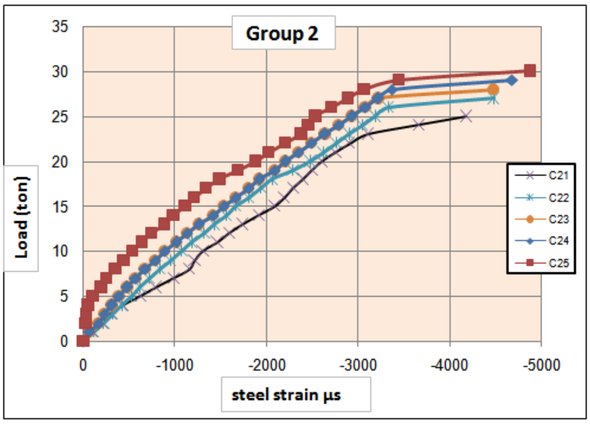

Figure 19 Comparison between longitudinal Steel strain at midpoint for group 2

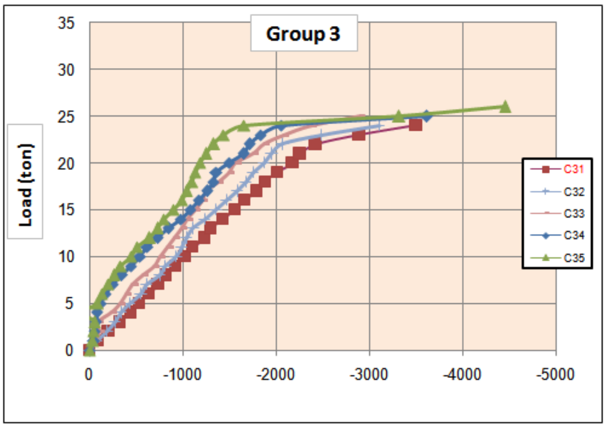

Figure 20 Comparison between longitudinal Steel strain at midpoint for group 3

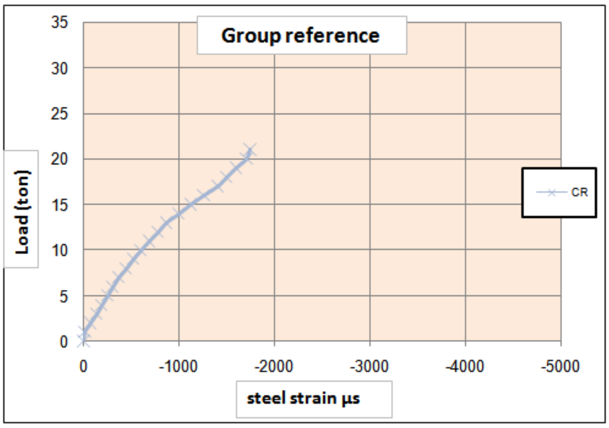

Figure 21 Comparison between longitudinal Steel strain at midpoint for group ref.

4.3 SMA Strains

The SMA strains at the midpoint were obtained from the electrical strain gauges. Figures (22) to (24) show the load SMA strain curves, through the load history.

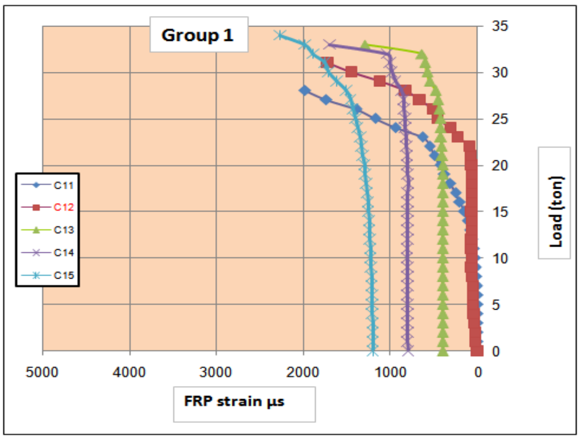

Figure 22 Comparison between longitudinal SMA strain at midpoint for group 1

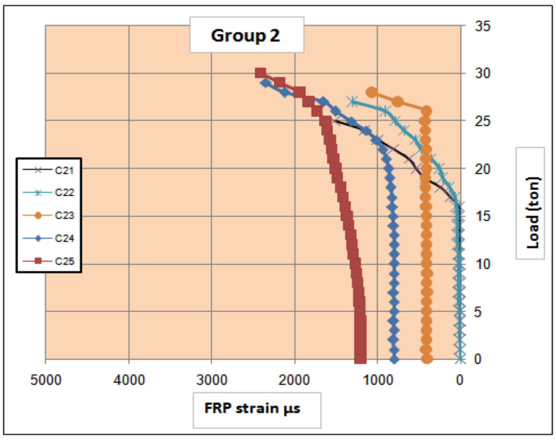

Figure 23 Comparison between longitudinal SMA strain at midpoint for group 2

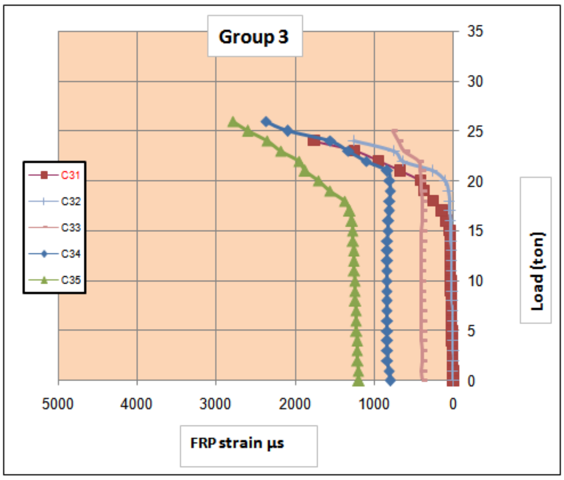

Figure 24 Comparison between longitudinal SMA strain at midpoint for group 3

5. Conclusions

The present study investigated the effect of active and passive confined external stirrups on capacity of RC columns. The following summarizes the findings of this investigation:

1) The increase in the spacing between passive and active external stirrups causes the decrease of the capacity of columns strengthened with SMA.
2) The increase tension force in the external stirrups caused the increase of the capacity of columns strengthened with SMA.
3) The increase temperature external stirrups caused the increase of the capacity of columns strengthened with SMA.
4) For the passive external stirrups, the experimental failure load was nearly equal the analytical (ACI) failure load.

References

1) ACI Committee 318, Building Code Requirements for Reinforced Concrete (ACI 318-2008) and Commentary (ACI 318R-2008), American Concrete Institute.
2) ACI Committee 440-2008, “Guide for the Design and Construction of Externally Bonded FRP Systems for Strengthening Concrete Structures”, Design Guidelines.
3) Chithra R , and Thenmozhi R. “Strength and ductility of concrete cylinders reinforced with prefabricated steel cage“. International Journal of Engineering Science and Technology (IJEST), 2011; 09: 6930- 6939.
4) Choi et al. “The behavior of concrete cylinders confined by shape memory alloy wires ” IOP Publishing Ltd (2008)
5) Jose M. Adam, Pedro A. Caldern and Francisco J. Pallarés, “Design strength of axially loaded RC columns strengthened by steel caging” Materials and Design 4069–4080. 30 (2009)
6) E.C.P. 208/2005 Egyptian Code of Practice for Design and Applications of FRP, Ministry of Development, New Communities, Housing and Utilities, National Housing and Building Research Center.
7) Mander, J. B., Priestley, M. J. N. and Park, R. “Theoretical stress-strain model for confined concrete. J. Struct. Eng. Div., ASCE, 1988, 114 (8), pp 1805-1826.
8) Matthys S., Toutanji H. and Gilbert J. “Behavior of Large-Scale Rectangular Columns Confined with FRP Composites”, Journal of structural engineering © ASCE. 62-71. JANUARY/FEBRUARY 2010.
9) Moghaddam H., Samadi M., Mohebbi S. and Pilakoutas K. “Compressive behavior of concrete actively confined by metal strips, part B: analysis” , Materials and Structures (2010) 43:1383–1396
10) Nesheli K.N. et.al.” External Prestressing Concrete Columns with Fibrous Composite Belts” FRPRCS-7 1631-1646 (2004).
11) Saatcioglu M. et.al. ‘‘Rectangular concrete columns retrofitted by external prestressing for seismic shear resistance’’ 13th World Conference on Earthquake Engineering Vancouver, B.C., Canada Paper No. 2720 August 1-6, 2004